ORIGINAL ARTICLE
https://doi.org/10.4046/trd.2017.0124
ISSN: 1738-3536(Print)/2005-6184(Online) • Tuberc Respir Dis, Respir Dis 2019;82:133-142

Bleomycin Inhibits Proliferation via Schlafen-Mediated Cell Cycle Arrest in Mouse Alveolar Epithelial Cells

Soojin Jang, M.S.[1], Se Min Ryu, M.D., Ph.D.[1], Jooyeon Lee, M.S.[1], Hanbyeol Lee, M.S.[1], Seok-Ho Hong, Ph.D.[2], Kwon-Soo Ha, Ph.D.[3], Won Sun Park, Ph.D.[4], Eun-Taek Han, Ph.D.[5] and Se-Ran Yang, D.V.M., Ph.D.[1]

Departments of [1]Thoracic and Cardiovascular Surgery, [2]Internal Medicine, [3]Molecular and Cellular Biochemistry, [4]Physiology, and [5]Medical Environmental Biology and Tropical Medicine, Kangwon National University School of Medicine, Chuncheon, Korea

Background: Idiopathic pulmonary fibrosis involves irreversible alveolar destruction. Although alveolar epithelial type II cells are key functional participants within the lung parenchyma, how epithelial cells are affected upon bleomycin (BLM) exposure remains unknown. In this study, we determined whether BLM could induce cell cycle arrest via regulation of Schlafen (SLFN) family genes, a group of cell cycle regulators known to mediate growth-inhibitory responses and apoptosis in alveolar epithelial type II cells.

Methods: Mouse AE II cell line MLE-12 were exposed to 1–10 μg/mL BLM and 0.01–100 μM baicalein (Bai), a G1/G2 cell cycle inhibitor, for 24 hours. Cell viability and levels of pro-inflammatory cytokines were analyzed by MTT and enzyme-linked immunosorbent assay, respectively. Apoptosis-related gene expression was evaluated by quantitative real-time reverse transcription-polymerase chain reaction (qRT-PCR). Cellular morphology was determined after DAPI and Hoechst 33258 staining. To verify cell cycle arrest, propidium iodide (PI) staining was performed for MLE-12 after exposure to BLM.

Results: BLM decreased the proliferation of MLE-12 cells. However, it significantly increased expression levels of interleukin 6, tumor necrosis factor α, and transforming growth factor β1. Based on Hoechst 33258 staining, BLM induced condensation of nuclear and fragmentation. Based on DAPI and PI staining, BLM significantly increased the size of nuclei and induced G2/M phase cell cycle arrest. Results of qRT-PCR analysis revealed that BLM increased mRNA levels of BAX but decreased those of Bcl2. In addition, BLM/Bai increased mRNA levels of p53, p21, SLFN1, 2, 4 of Schlafen family.

Conclusion: BLM exposure affects pulmonary epithelial type II cells, resulting in decreased proliferation possibly through apoptotic and cell cycle arrest associated signaling.

Keywords: Idiopathic Pulmonary Fibrosis; Alveolar Epithelial Cells; Cell Cycle Arrest; Schlafen; Bleomycin

Address for correspondence: Se-Ran Yang, D.V.M., Ph.D.
Department of Thoracic and Cardiovascular Surgery, Kangwon National University School of Medicine, 1 Gangwondaehak-gil, Chuncheon 24341, Korea
Phone: 82-33-250-7883, **Fax:** 82-33-255-8809
E-mail: seran@kangwon.ac.kr
Received: Dec. 12, 2017
Revised: Mar. 20, 2018
Accepted: Apr. 30, 2018
Published online: Jun. 19, 2018

Introduction

Idiopathic pulmonary fibrosis (IPF) is the irreversible form of the idiopathic interstitial pneumonia that has symptoms of chronic and progressive dyspnea by unknown causes[1,2]. IPF is etiologically characterized with alveolar epithelial cell injury, fibroblast/myofibroblast proliferation, and excessive extracellular matrix (ECM) deposition leading to the destruction of the alveolar structure. Recently, the incidence and prevalence of IPF have been increased with emerging medical attention in public. In addition, environmental factors including stone, sand, silica, cigarette smoke and wood/metal/micro dust are seriously considered to IPF associated risk factors[3-5]. Those

risk factors cause the release of pro-inflammatory cytokines, ECM deposition leading to irreversible alveolar destruction[6]. Representatively, pirfenidone and nintedanib have been evaluated in clinical trials of patient with IPF due to anti-fibrotic effect, however, these therapeutics exhibit the context of certain limitations regarding safety and specific efficacy[7,8]. Although the pathogenesis of IPF which is associated with progressive fibro-proliferative as well as destructive pathway of alveolar epithelial cell, the underlying mechanism is still unknown.

Bleomycin (BLM) is a glycopeptide antibiotic with potent tumor therapeutic in various squamous carcinoma of testicular and lymph nodes. However, its adverse effect has been associated with lung injury. BLM-induced pulmonary toxicity is chemotoxic related to pulmonary fibrosis with symptoms of irregular respiration and cough[9,10]. In this aspect, the animal and cellular models of BLM induced lung fibrosis injury have been widely used due to the cytotoxic effects. In pulmonary parenchyma of IPF, alveolar epithelial cells have been considered as primary damaged cells of surrounding inflammatory[11]. Sisson et al.[12] has been reported that alveolar epithelial type II cells (AE II) in diphtheria toxin-exposed mouse lung functionally inhibited fibroblast proliferation and collagen synthesis. Moreover, BLM has promoted the release of pro-inflammatory cytokines such as tumor necrosis factor α (TNF-α), interleukin-6 (IL-6), and transforming growth factor β1 (TGF-β1)[13]. It has been generally accepted that fibrotic diseases are promoted by TGF-β1 and appear AE II cells apoptosis, accumulation of collagen and ECM, and fibroblast proliferation[10,14]. Emodin, an antibacterial anthraquinone exhibited the down-regulation of anti-apoptotic protein Bcl2 and up-regulation of pro-apoptotic protein BAX promoted apoptosis in TGF-β1–stimulated human fibroblasts[15]. In addition, BLM-induced DNA double-strand breaks increased expression of the p21/p53 pathway that involved cell cycle arrest and cell apoptosis[16]. Recently, Schlafen (SLFN) family are proteins that have biological functions the effect that regulation of lymphocyte differentiation, growth and T-cell development/activation[17]. It has been reported that SLFN family have regulation of cell cycle progression and growth arrest[18,19]. Baicalein (Bai) induced G1 cell cycle arrest and apoptosis in osteosarcoma cell[20]. Moreover, Bai induced G1/G2 cell cycle arrest in rat heart endothelial cells[21]. We used Bai in order to inhibit G1/G2 cell cycle of MLE-12 cells. Therefore, in this study, we determined whether SLFN family is involved in the regulation of cell proliferation and apoptosis in BLM or Bai exposed mouse AE II (MLE-12 cells).

Materials and Methods

1. Chemicals

BLM was purchased from Tokyo Chemical Industry (#B3972; Tokyo, Japan). Methylthiazolyldiphenyl-tetrazolium bromide (MTT) were bought from Sigma-Aldrich (#M5655; St. Louis, MO, USA). Hoechst 33258 were bought from Sigma-Aldrich (#94403). Bai was purchased from Sigma-Aldrich (#465119).

2. Cell culture and treatment

MLE-12 cells (#CRL-2110; American Type Culture Collection, Manassas, VA, USA) maintained in DMEM/F-12 (#SH30023.1; HyClone, South Logan, UT, USA) with 2% fetal bovine serum (FBS; #FBSUS500-S; AusGeneX, CA, Santa Clara, USA), 1% penicillin/streptomycin, 0.005 mg/mL insulin, 30 nM Sodium selenite, 10 nM Hydrocortisone, and 10 nM β-estradiol and incubated in incubator (37°C, 95% air/5% CO_2). MLE-12 cells maintained FBS-free media at 12 hours before BLM treatment. After starvations, BLM treated dose of 1–10 μg/mL for 24 hours in MLE-12 cells. Bai dissolved in dimethyl sulfoxide (DMSO) and treated dose of 0.01–100 μM for 24 hours in MLE-12 cells.

3. MTT assay

MLE-12 cells were grown in a 96-well plate and it was treated BLM or Bai for 24 hours. After treatment, 20 μL/mL of MTT reagent were added 100 μL per well for 2 hours at 37°C. The reagent was removed and each well was added 100 μL of DMSO and dissolved purple formazan crystals. The measurement was wavelength 570 nm of absorbency using microplate reader (BioTek, Winooski, VT, USA). Calculation of cell viability was divided BLM treatment group into non-treatment.

4. Quantitative real-time reverse transcription-polymerase chain reaction

Total RNA from MLE-12 cells was isolated using Trizol Isolation Reagent (#79306; Qiagen, NRW, Düsseldorf, Germany). For reverse transcription–polymerase chain reaction, 1 μg of total RNA was reverse transcribed for cDNA synthesis in each tube using Revers Transcription-premix (#EBT-1514; Elpis Biotech, Daejeon, Korea). Quantitative real-time reverse transcription–polymerase chain reaction (qRT-PCR) was used with SYBR Green (#RT501; Enzynomics, Daejeon, Korea) for gene expression of mRNA levels. Two pairs of primers are shown in Table 1. Relative quantification of gene expression was normalized Ct values of β-actin each sample and calculated by $2^{-\Delta\Delta Ct}$ methods.

5. Enzyme-linked immunosorbent assay

After BLM treatment in MLE-12 cells for 24 hours were measured TNF-α (#DY410), IL-6 (#DY406), and TGF-β1 (#DY1679) cytokine levels. Measurement of cytokine level

Table 1. Sequences of the primers in the qRT-PCR analysis

Gene	Sequence (5′→3′)	Size (bp)	NM_number
Surfactant protein C (SPC)	F: GGA GCA CCG GAA ACT CAG AA	80	NM_011359
	R: CCA GTG GAG CCG ATG GAA		
Bcl-2–like protein 4 (BAX)	F: AGG ATG CGT CCA CCA AGA AG	80	NM_007527
	R: CCT CTG CAG CTC CAT ATT GCT		
B-cell lymphoma 2 (Bcl2)	F: GAA GGG CTT CAC ACC CAA ATC	80	NM_009741
	R: CTT CTA CGT CTG CTT GGC TTT GA		
Cyclin-dependent kinase inhibitor 1 (p21)	F: GAG GCA GAC CAG CCT GAC A	80	NM_007669
	R: CGT GGG CAC TTC AGG GTT T		
Tumor protein p53 (p53)	F: CAC CTC ACT GCA TGG ACG AT	80	NM_011640
	R: CAC TCG GAG GGC TTC ACT TG		
Proliferating cell nuclear antigen (PCNA)	F: GCA ACT TGG AAT CCC AGA ACA	80	NM_011045
	R: GGT CTC GGC ATA TAC GTG CAA		
Schlafen 1 (SLFN1)	F : CCT ACC CCT TCC CCA TGC T	80	NM_011407
	R: ACC ATC AGG GCG CGT ATT AT		
Schlafen 2 (SLFN2)	F : AAT CTT TGG GCT GCC TAT TGG	80	NM_011408
	R: CGG CGC TCA CTT GTA CAG AA		
Schlafen 4 (SLFN4)	F: CAA ACG CTG CCT GTC ACT CAC T	80	NM_011410
	R: GAT TTG TGC ACT TCG ATG AAT TTG		
β-Actin	F: AGG CCA ACC GTG AAA AGA TG	80	NM_007393
	R: CAC AGC CTG GAT GGC TAC GT		

qRT-PCR: quantitative real-time reverse transcription–polymerase chain reaction.

was used DuoSet enzyme-linked immunosorbent assay kit (R&D Systems, Minneapolis, MN, USA) in MLE-12 cell culture supernatant. All data were obtained duplicated experiments repeated at least three.

6. Hoechst 33258 staining

MLE-12 cells were grown at on sterile cover glass and treated BLM for 24 hours. The culture medium was removed through suction and the cells were washed that used with phosphate buffered saline. The cells were fixed with 4% paraformaldehyde for 10 minutes at room temperature (RT) and permeabilized with 0.2% Tripton X-100 for 10 minutes at RT. The cells were incubated with 1 μg/mL Hoechst 33258 for 10 minutes at 37°C and were mounted on the slide. Photographs were observed using a fluorescence microscope (Olympus, Tokyo, Japan). The abnormal index was measured by and calculated percentages (%).

7. Immunocytochemistry

MLE-12 cells were grown at on sterile cover glass and treated BLM for 24 hours. The cells were fixed with 4% paraformaldehyde for 10 minutes, permeabilized with 0.2% Tripton X-100 for 10 minutes. The cells were stained nuclei with DAPI (#F6057; Sigma-Aldrich). Photographs were studied using a confocal laser-scanning microscope (#LSM 510; Carl Zeiss, Stuttgart, Germany). The nuclear size was obtained by nuclear area measured using ImageJ.

8. Propidium iodide staining

The cells were grown at 6-well plate and treated BLM for 24 hours. The cells harvested and fixed in 70% ethanol for 15 minutes at –20°C. DNA staining was using propidium iodide (PI) staining reagent (#550825; BD Sciences, San Jose, CA, USA) for 15 minutes at RT. Results were analyzed using Flow Cytometry (Accuri C6; BD Biosciences).

9. Statistical analysis

All results were shown as the mean±standard deviation. One-way analysis of variance (ANOVA) was calculated for comparisons of multiple groups and Dunnett's test was used by *post hoc* test. Statistically significant was considered the value of $p<0.05$, $p<0.01$, and $p<0.001$. All results were analyzed

using Prism 5 and repeated experiments at least three.

Results

1. BLM increased pro-inflammatory cytokines with loss of cell viability

In order to determine whether BLM affects cellular proliferation, MLE-12 cells were treated with BLM (1–10 μg/mL) for 24 hours. The morphological change occurred flatten and enlargement of cell body in MLE-12 cells exposed to BLM under the microscope (Figure 1A). In MTT assay, cell viability was significantly decreased in treatment up to 10 μg/mL BLM (Figure 1B). In qRT-PCR analysis, mRNA level of surfactant protein C (SPC) which is a specific marker of lung AE II cell was decreased (Figure 1C). Moreover, pro-inflammatory cytokines including TNF-α, IL-6, and TGF-β1 were significantly released in response to BLM treatment in MLE-12 cells (Figure 1D–F).

2. BLM-induced apoptosis and cell cycle arrest with nuclear enlargement

We determine whether BLM induces apoptosis and cell cycle arrest in MLE-12 cells. In Hoechst 33258 staining, the nucleus of BLM treated MLE-12 cells were occurred condensation and fragmentation in a dose-dependent manner under the microscope (Figure 2A). Moreover, in qRT-PCR analysis, BLM treatment increased mRNA expression of a

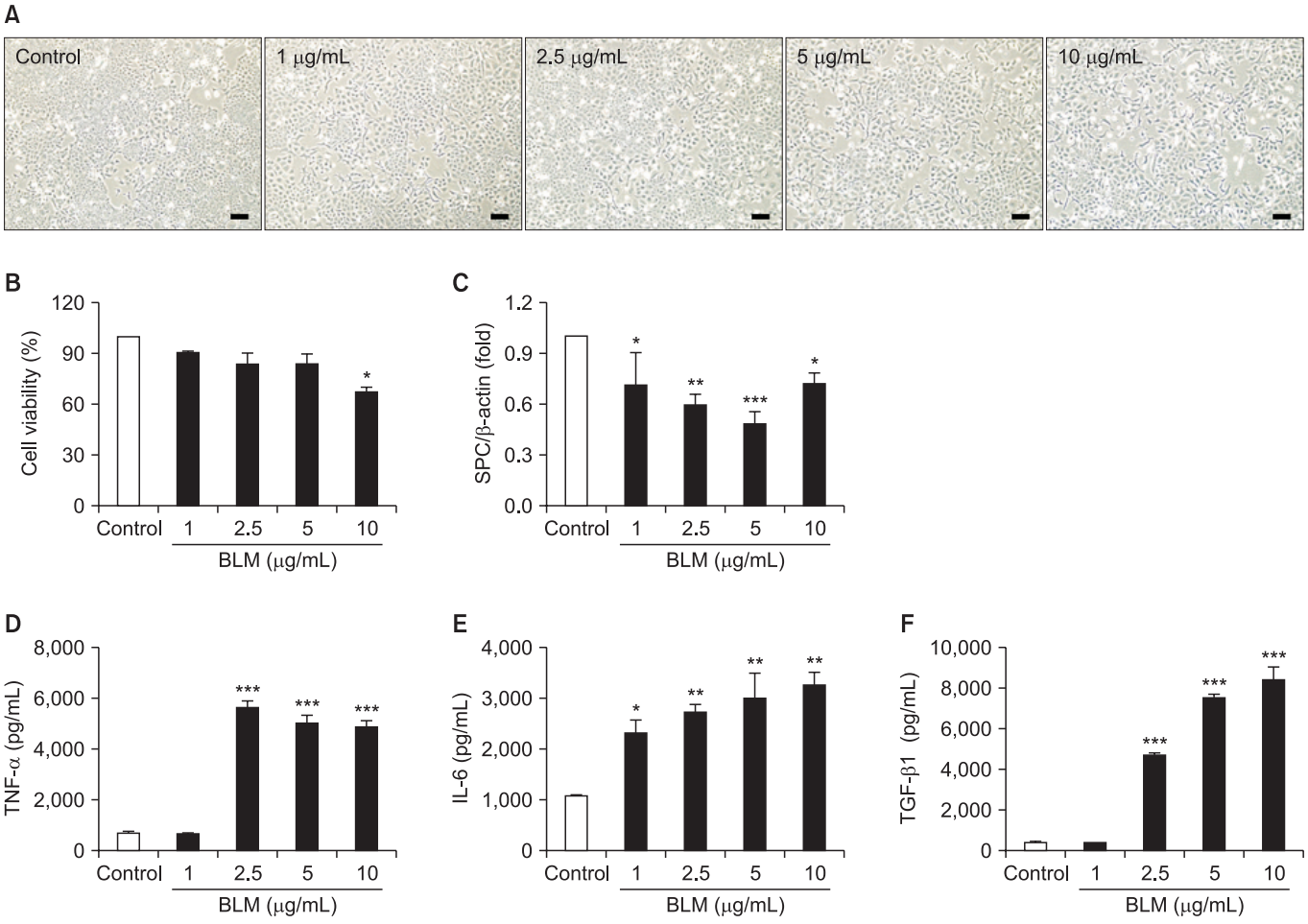

Figure 1. In the MLE-12 cells was evaluated toxicity effects of by bleomycin (BLM). MLE-12 cells were treated BLM (1–10 μg/mL) for 24 hours. (A) MLE-12 cells were induced morphological change by BLM. Scale bars=100 μm. (B) MLE-12 cells were treated with BLM and determined cell viability using MTT assay. (C) Expression of alveolar epithelial cell marker, surfactant protein C (SPC) was measured by quantitative real-time reverse transcription–polymerase chain reaction. The graph was measured inflammatory cytokines of tumor necrosis factor α (TNF-α) (D), interleukin-6 (IL-6) (E), and transforming growth factor β1 (TGF-β1) (F) in cell culture supernatant in enzyme-linked immunosorbent assay. *p<0.05, **p<0.01, ***p<0.001.

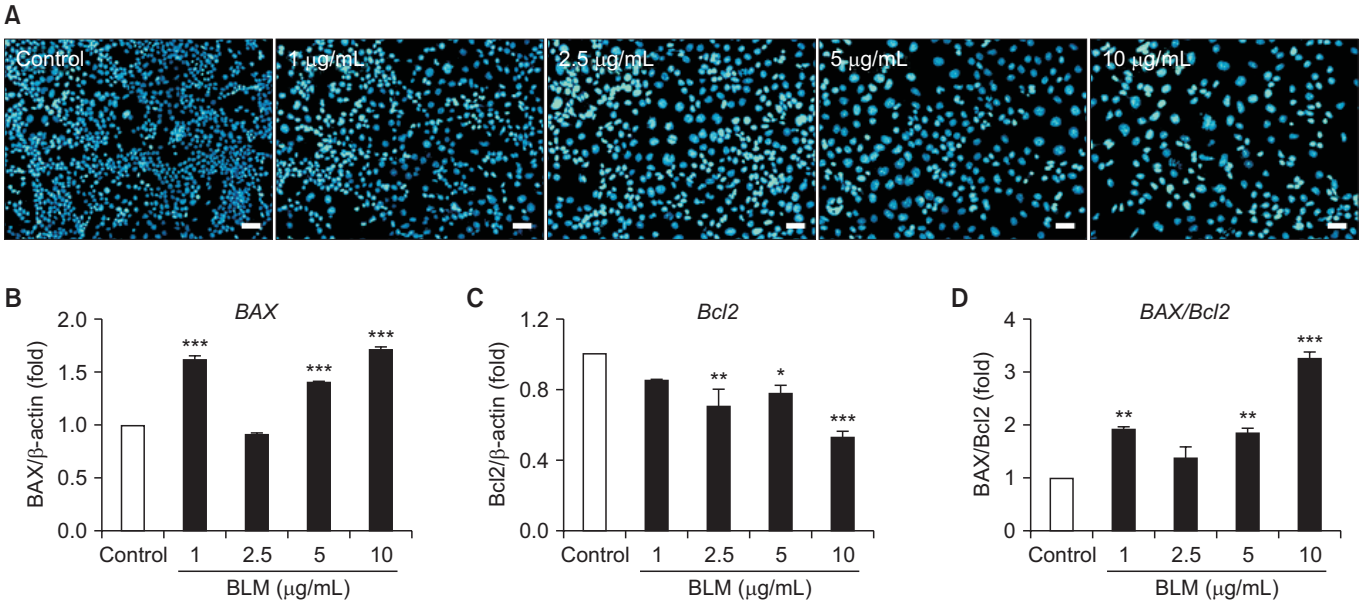

Figure 2. The MLE-12 cells induced apoptosis by bleomycin (BLM). (A) MLE-12 cells were stained with Hoechst 33258 staining after BLM treatment for 24 hours. Scale bars=100 μm. Expression of cell apoptosis marker, BAX (B) and Bcl2 (C) was measured by quantitative real-time reverse transcription-polymerase chain reaction (qRT-PCR). BAX/Bcl2 ratio (D) was divided (B, C) that measured by qRT-PCR. *p<0.05, **p<0.01, ***p<0.001.

pro-apoptotic factor (BAX) while decreased expression of anti-apoptotic factor (Bcl2) (Figure 2B). Cell cycle arrest was analyzed using DAPI and PI staining. In DAPI staining, cellular nucleus enlargement was morphologically found with loss of cell number (Figures 2A, 3A, B). It has been shown that increased size of nucleus is associated with cell cycle arrest leading to senescence[22]. Therefore, we measured nuclear size and the abnormal index. As a result, nucleus size and abnormal index were significantly increased in BLM exposed in MLE-12 cells (Table 2). In addition, in flow cytometry analysis, BLM decreased G0/G1 whereas increased S and G2/M phase in MLE-12 cells (Figure 3B). These findings suggest that BLM increased nuclear enlargement and it is associated with apoptosis and cell cycle arrest.

3. BLM-mediated the alteration of cell cycle regulatory gene expression in MLE-12 cells

We next determined the alteration of cell cycle arrest-related gene by BLM treatment for 24 hours in MLE-12 cells. In qRT-PCR analysis, the mRNA levels of *p21* and *p53* were significantly increased whereas the mRNA level of *Pcna* was deceased in MLE-12 cells treated with BLM for 24 hours (Figure 4A, B). SLFN family has been implicated the cell cycle regulation and cell growth arrest[19]. Therefore, we conducted qRT-PCR analysis in BLM-exposed MLE-12 cells, and mRNA levels of *SLFN2* and *SLFN4* were significantly increased rather than the mRNA expression of *Slfn1* (Figure 4D–F). These data suggest that cell cycle arrest–related genes including *p21*, *p53*, and SLFN family are increased by BLM treatment leading to apoptosis in MLE-12 cells.

4. Bai-mediated the alteration of SLFN family gene expression in MLE-12 cells

To determine whether cell cycle arrest-related gene and SLFN family gene expression level were changed by Bai that G1/G2 phase cell cycle arrest inhibitor. The cell viability was significantly decreased by Bai in dose-dependent manner (Figure 5A). The mRNA level of cell cycle arrest-related gene such as *p21*, *p53*, *Slfn1*, *Slfn2*, and *Slfn4* were significantly increased by Bai (Figure 5B–F). These data suggest that SLFN1, SLFN2, and SLFN4 associated G1/G2 cell cycle arrest in MLE-12 cells.

Discussion

Injury of AE II cells has been implicated the pathological feature to trigger the loss of type I alveolar epithelial cells leading to induce the migration of activated fibroblasts in interstitial compartment of distal alveoli in the pathogenesis of pulmonary fibrosis[23]. Injury of AE II cells includes cellular functional deficiency such as decreased SPC expression which functions to decrease collagen accumulation and inflammation[24], increased secretion of pro-inflammatory cy-

https://doi.org/10.4046/trd.2017.0124

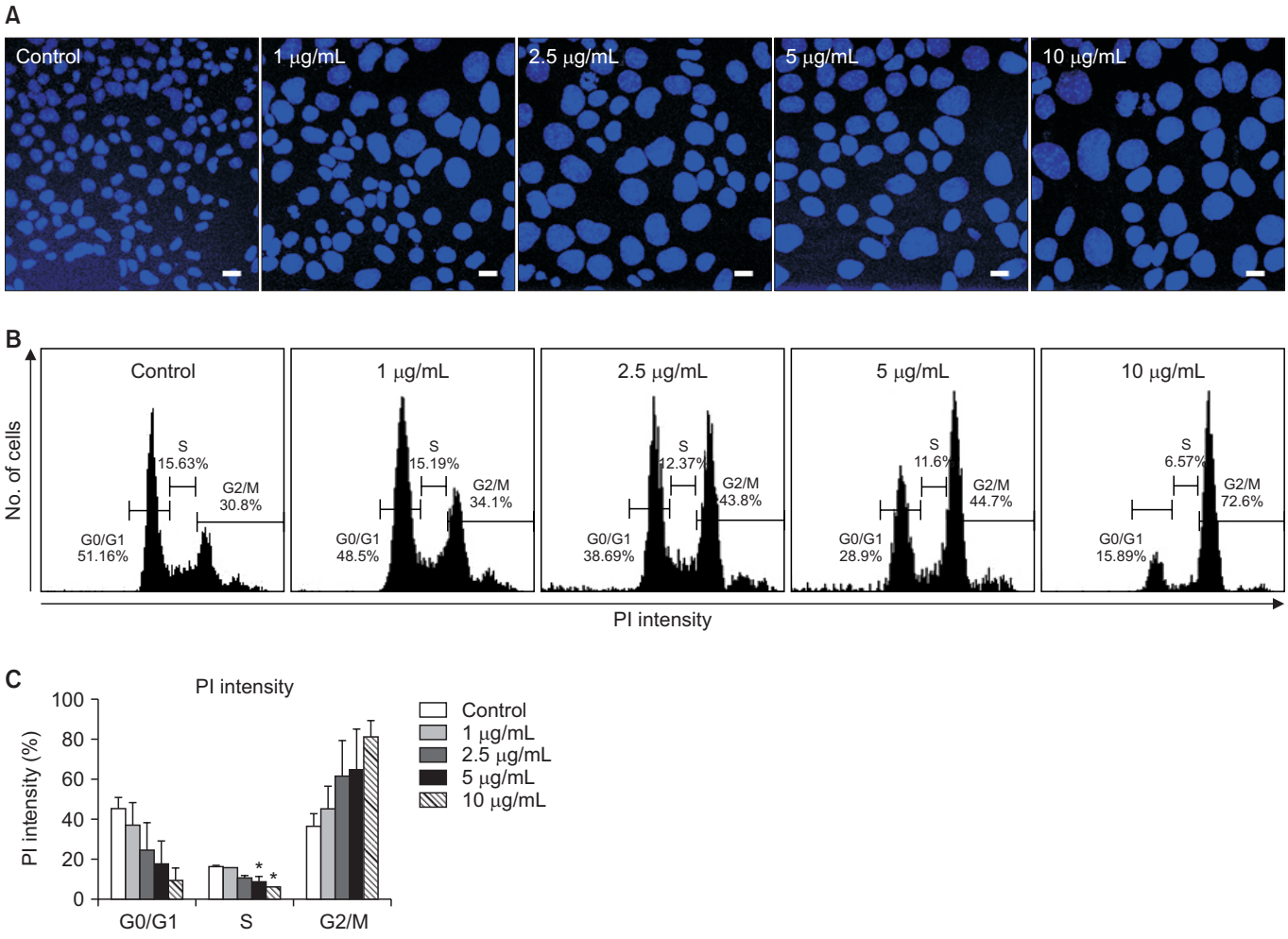

Figure 3. Evaluation of nuclear enlargement and cell cycle arrest induced in MLE-12 cells by bleomycin (BLM). (A) The image was obtained using DAPI staining in MLE-12 cells after BLM treatment. Scale bars=200 μm. (B) Propidium iodide (PI) staining was performed for cell cycle arrest in MLE-12 cells after BLM treatment. (C) Statistical analysis was each percentage of the field in the samples. *p<0.05.

Table 2. Nuclear size and apoptotic index by bleomycin treatment in MLE-12 cells

Group	Nucleus size (μm)	Abnormal index (%)†
Control	72.6	32.1
Bleomycin 1 μg/mL	136.5***	62.6**
Bleomycin 2.5 μg/mL	129.9***	90.0***
Bleomycin 5 μg/mL	128.3***	95.0***
Bleomycin 10 μg/mL	167.5***	88.6***

**p<0.01, ***p<0.001.
†Abnormal index was calculated by (nuclear fragmenet and enlargement cell/total cell number)×100 (%).

tokines[25], and accelerated the cellular senescence of alveolar epithelium[26]. In human A549 cell line and rat primary AE II cells treated with BLM, senescence-associated β-gal activity and flat/enlarged morphology has been exhibited[27]. In this perspective, the nuclear enlargement and decreased viability of AE II cells in our findings agree with BLM-induced cellular senescence. Moreover, cellular senescence accelerates to undergo cell cycle arrest with distinct morphological feature. Although the cellular senescence in tissue fibrosis is unclear, it is generally accepted that telomeres are shortened in AE II cells of IPF patients[28]. Recently, Naikawadi et al.[29] have been shown that deletion of telomere repeat binding factor 1 (TRF1) which is a component protein in shelterin complex of telomeres of AE II cells causes pulmonary fibrosis in SPC-CreTrf1$^{fl/fl}$ mice. When SPC-CreTrf1$^{fl/fl}$ mice are induced fibrosis, the prolonged telomere dysfunction caused AE II cell hyperplasia during lung remodeling. In contrast, Povedano et al.[30] demonstrated that Trf1 deletion develops 90% of AE II cells apoptosis and pulmonary fibrosis through induction of telomere damage using lungs of Trf1$^{\Delta/\Delta}$ mouse. In addition, Cui et al.[31] have been shown that up-regulated miR-34a alveolar epithelial dysfunc-

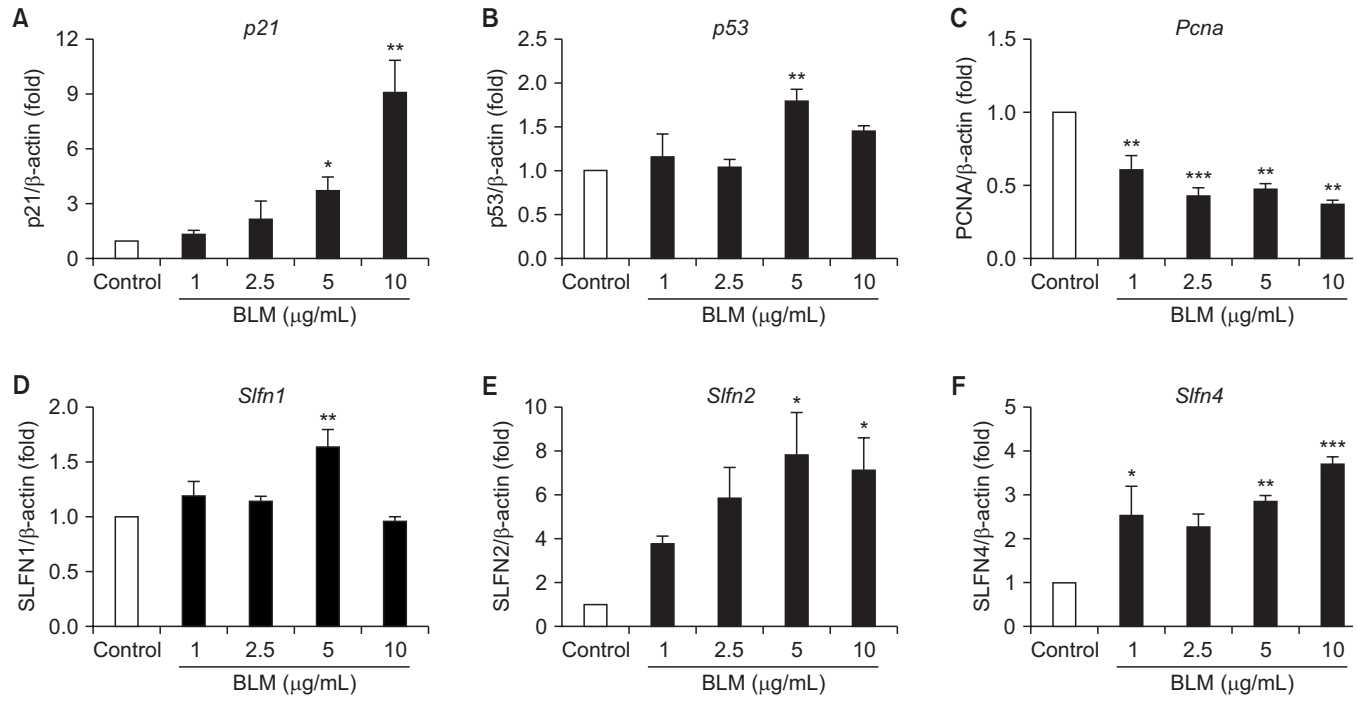

Figure 4. Gene expression associated with cell cycle of bleomycin (BLM) treatment in MLE-12 cells. The MLE-12 cells were treated with BLM (1–10 μg/mL) for 24 hours. Measured the *p21* (A), *p53* (B), and proliferating cell nuclear antigen (*Pcna*) (C) at the mRNA levels, which were associated with cell cycle. BLM exposed MLE-12 cells were measured expression of *Slfn1* (D), *Slfn2* (E), and *Slfn4* (F) by quantitative real-time reverse transcription–polymerase chain reaction analysis.

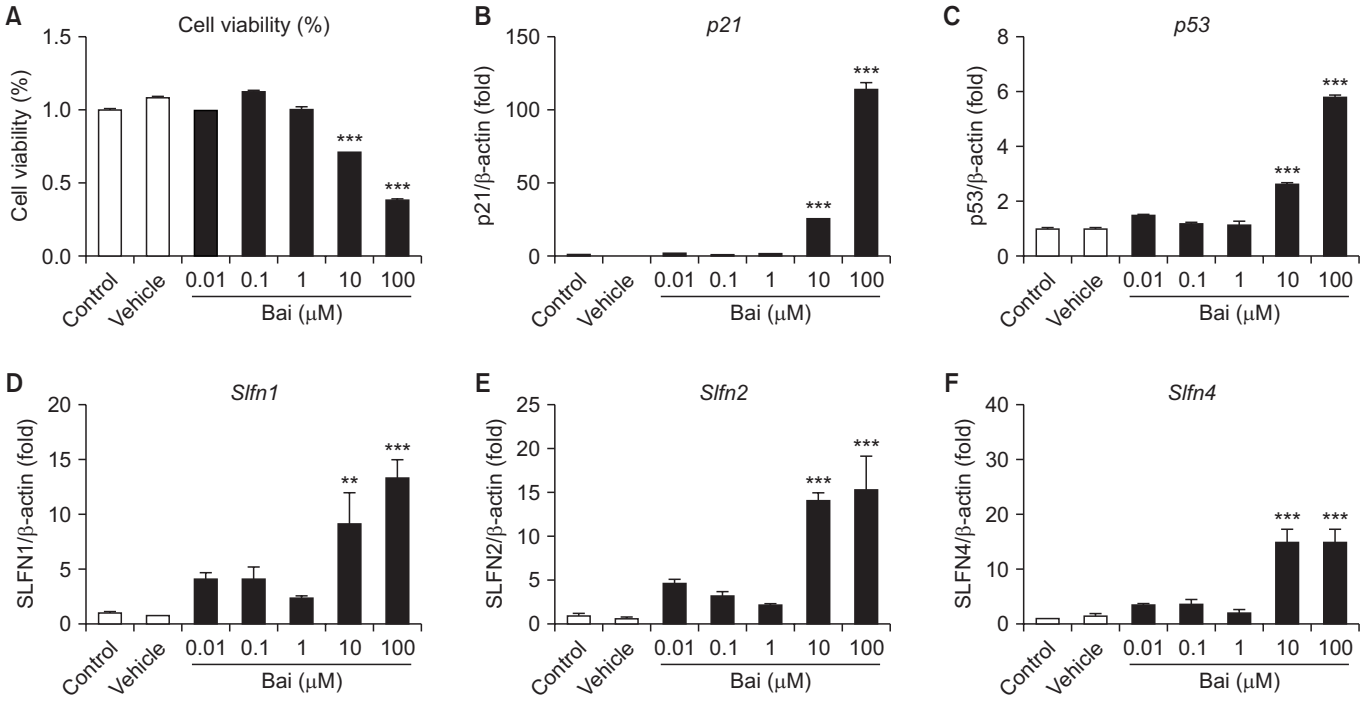

Figure 5. The evaluation of baicalein (Bai) affected MLE-12 cells. The MLE-12 cells were treated with Bai (0.01–100 μM) for 24 hours. (A) The cell viability was measured using MTT assay. Measured the *p21* (B) and *p53* (C) at the mRNA levels, which were associated with cell cycle. Bai exposed MLE-12 cells were measured expression of *Slfn1* (D), *Slfn2* (E), and *Slfn4* (F) by quantitative real-time reverse transcription–polymerase chain reaction analysis. **p<0.01, ***p<0.001.

https://doi.org/10.4046/trd.2017.0124

tion is associated with fibrotic lungs and lung myofibroblasts. MiR-34a did not have any obvious difference TGF-β1–induced myofibroblast differentiation; however, the underlied pathway is still conflicting. In this regard, apoptosis is one of roles to be allied in stress-induced morphological change and cellular aging. Accordingly, BLM mediated lung injury and/or pulmonary toxicity is well-known; however, the involved pathway is still remained. Brar et al.[32] have shown that oxidative stress causes mitochondrial/nuclear DNA damage and caspase3, poly(ADP-ribose) polymerase, BAX were increased leading to apoptosis in human alveolar epithelial A549 cells. Accordingly, our data agree with BLM-induced apoptosis including up-regulation of pro-apoptotic factor BAX and decreased anti-apoptotic factor Bcl2. Previously, we have shown that cigarette smoke extract similarly induced the apoptotic pattern of apoptosis-related protein family members (Bcl2 and BAX) in mouse lung tissue-derived fibroblasts[33]. In our data, regulation of Bcl2/Bax was significantly associated with alveolar epithelial cells and pulmonary fibroblasts.

After DNA damage increased p53 and p21 proceeds into a sustained arrest in cell cycle arrest in mammalian cells[34]. In colorectal cancer cells, the etoposide-induced nuclear enlargement happens strong G2/M phase cell cycle arrest in HCT116 cells[35]. Additionally, BLM-induced G2 phase cell cycle arrest in the human leukemia-derived cell line[36]. Our data have shown that BLM treatment induced G2/M phase arrest via nuclear enlargement leading to DNA damage in MLE-12 cells. Recently, Shetty et al investigated that suppression of p53 and miR-34a feedback validates as a potential therapeutic target in a mouse model of BLM, silica, and cigarette smoke exposure and sepsis-induced lung injury[37]. Aoshiba and colleagues reported that BLM-induced cellular senescence increased the level of p21 in an A549 human lung cancer cell[27]. Linge et al.[38] also have been reported that BLM-induced cell senescence increased the level of p21, p53, and caveolin-1 and occurred G2/M phase arrest. In this study, we have shown that the SLFN family has been included in BLM-mediated apoptosis of alveolar epithelial cells. Despite the diverse biological roles of SLFNs in mammals, it is unknown the associated cellular- and molecular- mechanisms in alveolar epithelial cells. In mouse embryonic fibroblasts, interferon (IFN) induced *Slfn* genes via STAT1 regulation[19]. As recent studies suggested, it seems that SLFNs play a critical role in the generation of IFN-inducible responses[17]. Brady et al.[39] have been shown that SLFN1 expression causes cell cycle arrest by inhibiting of mitogen-mediated cycle D1 level in murine CHO epithelial cell line. In our data, when MLE-12 cells were treated with BLM, mRNA levels of *Slfn1*, *Slfn2* and *Slfn4* were significantly increased. In addition, gene expression level of p21, p53, and SLFN1, SLFN2, SLFN4 in MLE-12 cells were increased by Bai. These observations suggest that increased SLFNs expression may associate with cell cycle arrest via regulation of p21/p53 in alveolar epithelial cells. Taken together, we determined that exposure of BLM increases of the release of a pro-inflammatory cytokine, nuclear enlargement, apoptosis and cell cycle arrest in MLE-12 cells. Accordingly, these findings suggest that pulmonary toxicity by BLM may induce DNA damage including SLFN family-related cell cycle arrest. Therefore, we determined whether SLFN family might be involved to understand the pathogenesis of pulmonary fibrosis.

Authors' Contributions

Conceptualization: Yang SR. Methodology: Lee H, Lee J. Formal analysis: Jang S. Data curation: Jang S. Software: Hong SH. Validation: Ha KS, Park WS, Han ET. Investigation: Ryu SM. Writing – original draft preparation: Jang S. Writing – review and editing: Yang SR. Approval of final manuscript: all authors.

Conflicts of Interest

No potential conflict of interest relevant to this article was reported.

Acknowledgments

This work was supported by the National Research Foundation of Korea (NRF) grant funded by the Korea government (NRF-2017R1A2B4006197, 2017M3A9B4051542, 2016R1A2A1A05004975) and Kangwon National University (No.520160459).

References

1. King TE Jr, Pardo A, Selman M. Idiopathic pulmonary fibrosis. Lancet 2011;378:1949-61.
2. Yao R, He Y, Zeng Z, Liang Z, Cao Y. Protective effect of adiponectin on paraquat-induced pulmonary fibrosis in mice. Mol Cell Toxicol 2015;11:247-55.
3. Borchers AT, Chang C, Keen CL, Gershwin ME. Idiopathic pulmonary fibrosis: an epidemiological and pathological review. Clin Rev Allergy Immunol 2011;40:117-34.
4. Hardie WD, Hagood JS, Dave V, Perl AK, Whitsett JA, Korfhagen TR, et al. Signaling pathways in the epithelial origins of pulmonary fibrosis. Cell Cycle 2010;9:2769-76.
5. Romero Y, Bueno M, Ramirez R, Alvarez D, Sembrat JC, Goncharova EA, et al. mTORC1 activation decreases autophagy in aging and idiopathic pulmonary fibrosis and contributes to apoptosis resistance in IPF fibroblasts. Aging Cell 2016;15:1103-12.
6. Tanaka Y, Ishitsuka Y, Hayasaka M, Yamada Y, Miyata K, Endo M, et al. The exacerbating roles of CCAAT/enhancer-binding

protein homologous protein (CHOP) in the development of bleomycin-induced pulmonary fibrosis and the preventive effects of tauroursodeoxycholic acid (TUDCA) against pulmonary fibrosis in mice. Pharmacol Res 2015;99:52-62.
7. Jablonski RP, Kim SJ, Cheresh P, Williams DB, Morales-Nebreda L, Cheng Y, et al. SIRT3 deficiency promotes lung fibrosis by augmenting alveolar epithelial cell mitochondrial DNA damage and apoptosis. FASEB J 2017;31:2520-32.
8. Puglisi S, Torrisi SE, Vindigni V, Giuliano R, Palmucci S, Mule M, et al. New perspectives on management of idiopathic pulmonary fibrosis. Ther Adv Chronic Dis 2016;7:108-20.
9. Hay J, Shahzeidi S, Laurent G. Mechanisms of bleomycin-induced lung damage. Arch Toxicol 1991;65:81-94.
10. Tang H, Gao L, Mao J, He H, Liu J, Cai X, et al. Salidroside protects against bleomycin-induced pulmonary fibrosis: activation of Nrf2-antioxidant signaling, and inhibition of NF-κB and TGF-β1/Smad-2/-3 pathways. Cell Stress Chaperones 2016;21:239-49.
11. Selman M, Pardo A. Role of epithelial cells in idiopathic pulmonary fibrosis: from innocent targets to serial killers. Proc Am Thorac Soc 2006;3:364-72.
12. Sisson TH, Mendez M, Choi K, Subbotina N, Courey A, Cunningham A, et al. Targeted injury of type II alveolar epithelial cells induces pulmonary fibrosis. Am J Respir Crit Care Med 2010;181:254-63.
13. Huang TT, Lai HC, Ko YF, Ojcius DM, Lan YW, Martel J, et al. Hirsutella sinensis mycelium attenuates bleomycin-induced pulmonary inflammation and fibrosis in vivo. Sci Rep 2015;5:15282.
14. Wang Y, Li R, Chen L, Tan W, Sun Z, Xia H, et al. Maresin 1 inhibits epithelial-to-mesenchymal transition *in vitro* and attenuates bleomycin induced lung fibrosis *in vivo*. Shock 2015;44:496-502.
15. Guan R, Wang X, Zhao X, Song N, Zhu J, Wang J, et al. Emodin ameliorates bleomycin-induced pulmonary fibrosis in rats by suppressing epithelial-mesenchymal transition and fibroblast activation. Sci Rep 2016;6:35696.
16. Okudela K, Ito T, Mitsui H, Hayashi H, Udaka N, Kanisawa M, et al. The role of p53 in bleomycin-induced DNA damage in the lung: a comparative study with the small intestine. Am J Pathol 1999;155:1341-51.
17. Mavrommatis E, Fish EN, Platanias LC. The schlafen family of proteins and their regulation by interferons. J Interferon Cytokine Res 2013;33:206-10.
18. Geserick P, Kaiser F, Klemm U, Kaufmann SH, Zerrahn J. Modulation of T cell development and activation by novel members of the Schlafen (slfn) gene family harbouring an RNA helicase-like motif. Int Immunol 2004;16:1535-48.
19. Katsoulidis E, Carayol N, Woodard J, Konieczna I, Majchrzak-Kita B, Jordan A, et al. Role of Schlafen 2 (SLFN2) in the generation of interferon α-induced growth inhibitory responses. J Biol Chem 2009;284:25051-64.
20. Zhang Y, Song L, Cai L, Wei R, Hu H, Jin W. Effects of baicalein on apoptosis, cell cycle arrest, migration and invasion of osteosarcoma cells. Food Chem Toxicol 2013;53:325-33.
21. Hsu SL, Hsieh YC, Hsieh WC, Chou CJ. Baicalein induces a dual growth arrest by modulating multiple cell cycle regulatory molecules. Eur J Pharmacol 2001;425:165-71.
22. Sadaie M, Dillon C, Narita M, Young AR, Cairney CJ, Godwin LS, et al. Cell-based screen for altered nuclear phenotypes reveals senescence progression in polyploid cells after Aurora kinase B inhibition. Mol Biol Cell 2015;26:2971-85.
23. Aoshiba K, Tsuji T, Kameyama S, Itoh M, Semba S, Yamaguchi K, et al. Senescence-associated secretory phenotype in a mouse model of bleomycin-induced lung injury. Exp Toxicol Pathol 2013;65:1053-62.
24. Lawson WE, Polosukhin VV, Stathopoulos GT, Zoia O, Han W, Lane KB, et al. Increased and prolonged pulmonary fibrosis in surfactant protein C-deficient mice following intratracheal bleomycin. Am J Pathol 2005;167:1267-77.
25. Yonezawa R, Yamamoto S, Takenaka M, Kage Y, Negoro T, Toda T, et al. TRPM2 channels in alveolar epithelial cells mediate bleomycin-induced lung inflammation. Free Radic Biol Med 2016;90:101-13.
26. Kato A, Okura T, Hamada C, Miyoshi S, Katayama H, Higaki J, et al. Cell stress induces upregulation of osteopontin via the ERK pathway in type II alveolar epithelial cells. PLoS One 2014;9:e100106.
27. Aoshiba K, Tsuji T, Nagai A. Bleomycin induces cellular senescence in alveolar epithelial cells. Eur Respir J 2003;22:436-43.
28. Alder JK, Chen JJ, Lancaster L, Danoff S, Su SC, Cogan JD, et al. Short telomeres are a risk factor for idiopathic pulmonary fibrosis. Proc Natl Acad Sci U S A 2008;105:13051-6.
29. Naikawadi RP, Disayabutr S, Mallavia B, Donne ML, Green G, La JL, et al. Telomere dysfunction in alveolar epithelial cells causes lung remodeling and fibrosis. JCI Insight 2016;1:e86704.
30. Povedano JM, Martinez P, Flores JM, Mulero F, Blasco MA. Mice with pulmonary fibrosis driven by telomere dysfunction. Cell Rep 2015;12:286-99.
31. Cui H, Ge J, Xie N, Banerjee S, Zhou Y, Liu RM, et al. miR-34a promotes fibrosis in aged lungs by inducing alveolar-epithelial dysfunctions. Am J Physiol Lung Cell Mol Physiol 2017;312:L415-24.
32. Brar SS, Meyer JN, Bortner CD, Van Houten B, Martin WJ 2nd. Mitochondrial DNA-depleted A549 cells are resistant to bleomycin. Am J Physiol Lung Cell Mol Physiol 2012;303:L413-24.
33. Lee H, Park JR, Kim EJ, Kim WJ, Hong SH, Park SM, et al. Cigarette smoke-mediated oxidative stress induces apoptosis via the MAPKs/STAT1 pathway in mouse lung fibroblasts. Toxicol Lett 2016;240:140-8.
34. Bunz F, Dutriaux A, Lengauer C, Waldman T, Zhou S, Brown JP, et al. Requirement for p53 and p21 to sustain G2 arrest after DNA damage. Science 1998;282:1497-501.
35. Kang K, Lee SB, Yoo JH, Nho CW. Flow cytometric fluorescence pulse width analysis of etoposide-induced nuclear en-

largement in HCT116 cells. Biotechnol Lett 2010;32:1045-52.
36. Kaneko M, Matsuda D, Ohtawa M, Fukuda T, Nagamitsu T, Yamori T, et al. Potentiation of bleomycin in Jurkat cells by fungal pycnidione. Biol Pharm Bull 2012;35:18-28.
37. Shetty SK, Tiwari N, Marudamuthu AS, Puthusseri B, Bhandary YP, Fu J, et al. p53 and miR-34a feedback promotes lung epithelial injury and pulmonary fibrosis. Am J Pathol 2017;187:1016-34.
38. Linge A, Weinhold K, Blasche R, Kasper M, Barth K. Down-regulation of caveolin-1 affects bleomycin-induced growth arrest and cellular senescence in A549 cells. Int J Biochem Cell Biol 2007;39:1964-74.
39. Brady G, Boggan L, Bowie A, O'Neill LA. Schlafen-1 causes a cell cycle arrest by inhibiting induction of cyclin D1. J Biol Chem 2005;280:30723-34.